Rainfall-induced landslides by deficit field matric suction in unsaturated soil slopes

Kim, Junghwan; Kim, Yongmin; Jeong, Sangseom; Hong, Moonhyun

2017

https://hdl.handle.net/10356/104488

https://doi.org/10.1007/s12665-017-7127-2

Rainfall-induced landslides by deficit field matric suction in unsaturated soil slopes

Junghwan Kim[1], Yongmin Kim[2], Sangseom Jeong[1], Moonhyun Hong[1]

[1]Department of Civil and Environmental Engineering, Yonsei University, 50 Yonsei-ro, Seodaemun-gu, Seoul 03722, Republic of Korea

[2]School of Civil and Environmental Engineering, Nanyang Technological University, Singapore 639798, Singapore

Correspondence to: Sangseom Jeong (+82-2-2123-2807)

Abstract. Landslides are mainly triggered by the deepening of the wetting band accompanied by a decrease in matric suction induced by the water infiltration. This paper reports rainfall-induced landslides in partially saturated soil slopes through a field study. A comprehensive case study on the 2011 Umyeonsan (Mt.) landslides was highlighted. The incident involves the collapse of unsaturated soil slopes under extreme-rainfall event. A fundamental study was carried out on the cause and mechanism of landslide. A number of technical findings are of interest, including the failure mechanism of a depth of soil and effect of groundwater flow; the downward velocity of wetting front and the upward velocity of groundwater level. Based on this, an integrated analysis methodology for a rainfall-induced landslide is proposed in this paper that incorporates the field matric suction for obtaining hydraulic parameters of unsaturated soil. The field matric suction is shown to govern the rate of change in the water infiltration for the landslide analysis with respect to an antecedent rainfall. Special attention was given to a one-dimensional infiltration model to determine the wetting band depth in the absence of the field matric suction. The results indicate that landslide activities were primarily dependent on rainfall infiltration, soil properties, slope geometries, vegetations, and groundwater table positions. The proposed methodology has clearly demonstrated both shallow and deep-seated landslides, and shows good agreement with the results of landslide investigations.

1 Introduction

Rainfall-induced landslides are common mass-movement processes in mountainous areas, particularly in areas covered by shallow soil deposit of different grading and origin. (Jeong et al., 2008; Cascini et al., 2010; Kim et al., 2017). Significant examples are frequently recorded in pyroclastic deposits in Central America (Capra et al., 2003) and New Zealand (Ekanayake and Philipps, 2002), in-situ weathered soils in Hong Kong (Take et al., 2004) and Japan (Wang et al. 2002), colluvial weathered deposits in Hong Kong (Fuchu et al. 1999) and Korea (Park et al, 2013). In particular, landslides of the flow-type (Hunger et al., 2001) represents a significant threat to lives, livelihoods and infrastructure in most mountainous areas. For example, when South Korea experienced record rainfall in June and July 2011, some 151 landslides occurred in the Umyeonsan Mt. region affecting 13 villages. These landslides significantly impacted society because the mountain is located in a central part of Seoul, South Korea.

1

The triggering mechanisms of natural hill-slopes frequently comprise a complex interaction between hydrological and geotechnical processes, which in turn depends on irregular topography, hydro-geotechnical contexts by properties, boundary conditions such as permeability and the initial state of the slope (Sorbino and Nicotera, 2013). One of the most frequent triggering factors is represented by rainfall that can directly infiltrate the slope surface or can indirectly provide groundwater

5   supplies from the bedrock or aquitard (Kim et al., 2014). From a geotechnical perspective, the main reason for slope failure is the loss of matric suction and hence a loss of effective stress as water infiltrates the soil. Many researchers (Fredlund et al., 2012; Jeong et al., 2008; Kim et al., 2014) have studied rainfall-induced landslides through laboratory and field tests, as well as through numerical analysis. They have presented a mechanism for rainfall-induced landslides that commonly occur when the wetting bands progress into the soil, resulting in a loss of suction and a reduction in effective stress. According to related

10   studies by Rahardjo et al. (1998), Ng et al. (2003, 2008) and Jeong et al. (2008), landslides are commonly triggered by external stimuli, including modified slope stability conditions, increasing stress or reductions in strength. A matric suction range between 0 and 200 kPa is suggested as the range where the residual state can be determined for gravels, sand, and silts, whereas higher matric suction ranges of 500 to >1500 kPa are suggested for clays (Vanapalli et al., 1996). In particular, the measurements of maximum matric suction in the field during dry period is crucial in determining the stability of a slope.

15   Some attempts have been conducted to investigate a slope stability on a regional scale by GIS-based physical models (e.g., SINAMP, TRIGRS, and YS-SLOPE models) that incorporate rainfall infiltration, groundwater table variation, and unsaturated characteristics by simplifying the complex boundary conditions. However, these models are not appropriate to assess the failure mechanism of rainfall-induced landslides in unsaturated soil due to many assumptions and simplifications. Therefore, , the susceptibility analysis of rainfall-induced landslides on a large scale is usually performed using deterministic methods such as

20   the Limited Equilibrium Method (LEM) and Finite Element Method (FEM). They are significant in determining the cause and mechanism for slope failure by modeling slope geometry, the mechanical properties, permeability, and equilibrium condition. Commercial software such as GEO-SLOPE (2012), PLAXIS (2012), and SOIL-WORKS (2014) are widely used for simulating the seepage problem and slope stability (Lu et al., 2013; Costa and Sagaseta, 2010; Lee et al., 2012). Where a major part of the slip surface is below the groundwater table, the shear strength contribution from negative pore-water pressures above the

25   groundwater table is often ignored by setting their magnitudes to zero. However, in situations where the ground water table is deep or there is concern over the possibility of a shallow failure surface, negative pore water pressures can no longer be ignored (Fredlund an Rahardjo, 1995, Jeong et al., 2008; Kim et al., 2016).

This paper reports rainfall-induced landslides in partially saturated soil slopes through a field study. A comprehensive case study on the 2011 Umyeonsan (Mt.) landslides was highlighted. A fundamental study was carried out to investigate the cause

30   and mechanism of landslides in terms of rainfall, vegetation, and geotechnical characteristics. The monitoring of field matric suction was carried out to develop an integrated analysis methodology for the rainfall-induced landslide that incorporates the field matric suction for obtaining hydraulic parameters of unsaturated soil. Special attention was given to a one-dimensional infiltration model to determine the wetting band depth in the absence of the field matric suction. In combination of

2

comprehensive experimental and numerical studies, the observation gives insight to understand the mechanism of rainfall-induced landslides and the relative importance in inducing instability of unsaturated soil slopes.

2 Study Area

2.1 Geological framework

The study area of Mt. Umyeonsan is located in the central part of Seoul, Korea (Fig. 1). This site is positioned at latitude of 37°28'2"N and longitude of 127°0'25"E with an elevation of approximately 50 to 312.6 m above sea level. The area is underlain by metamorphic Precambrian gneissic rocks that belong to the Gyeonggi massif (Fig. 2). The bedrock mineralogy is primarily composed of plagioclase, quartz, biotite, feldspar and amphibole. The colluvial deposit consists of a poorly sorted mixture of sands and gravels in a silty matrix. The colluvium is directly associated with the origin and development of mass movement in this area. The bedrock is heavily fractured, intensely weathered, and covered by a layer of colluvium varying in thickness from a few centimeters to 13 m.

2.2 Regional framework

The Umyeonsan region is situated in the temperate monsoon zone which is generally hot and humid with abundant rainfall events in the summer. The annual average precipitation ranges between 1,100 and 1,500 mm, and 70% of the average falling in rainy season that lasts while June to September. In this area, small landslides frequently occur during the rainy season. The most catastrophic recorded landslides and debris flows occurred on Mt. Umyeonsan on July 27th of July, 2011. The intensity of this event is, to some extent, attributable to climate change, in terms of the higher intensity and longer duration of rainfall not only in the Umyeonsan region but also in the majority of the regions in Korea (Kim et al. 2012; Le and Bae 2013).

The catastrophic events that hit the Umyeonsan region are concentrated along the ridgeline of the mountain where slopes are steepest. The slope soil has low strength and low density. Debris flows with features are found, which are widely incised by gullies. They were similar to fluid flow and the volume was increased by eroding the ground. Among twenty watersheds, a catastrophic landslide watershed, the Raemian and Deokuam (W1 and W20 in Fig. 3), were selected as a study.

The morphological characteristics of the Umyeonsan region (Korean Geotechnical Society, 2012) are characterized by a series of watersheds with surface areas ranging from 17,700 to 786,400 m^2, channel gradient generally less than 22 degrees and a maximum runout distance of all debris flows of 1,365 m. Individual watersheds contain up to 30 landslides and these form the main source of the debris flow development. The mobilized volume ranges from 8 to 1,827 m^3 in each gully. The Raemian watershed (W1 of the study area) has the largest debris flow volume of 1,827 m^3, some 52% of the total landslide volume. Landslides are initiated at slope angles ranging from 16 to 44° and some 60% of all landslides occurred at slope angles greater than 30°. It can therefore be concluded that most debris flows will also originate at slope angles close to 30°and this observation is supported at other sites (Tiranti et al. 2008). Field surveys revealed that landslide and debris flow in the Umyeonsan region were developed by three main processes: 1) initial failure produces a shallow landslide trace caused by the transitional sliding

of the loose colluvium overlying gneiss bedrock (Fig. 4a). 2) with the incorporation of surface water runoff resulting from intensive rainfall, the soil slides mobilize completely to form debris flows; 3) overland flow in rills on the valley slope is gradually concentrated in the gully, which then easily erodes the loose debris flow deposits and ran rapidly downhill in relatively narrow channels. The latter process is described as the fire hose effect (Godt and Coe, 2007). The depth of these channels varied from 0.1 to 1.5 m, and the base of the gullies was located within the colluvial layer or along the interface between the colluvium and bedrock (Fig. 4b). The gneiss bedrock, where exposed, was deeply fractured and highly weathered (Fig. 4c). Transported debris flow were deposited at the confluence of the gullies and the toe of the mountain. The debris flow material typically comprised of soil, rock, woody blocks and and water (Fig. 4d).

3 Experimental tests and field matric suction monitoring

To identify the geotechnical processes acting in the soils of the Umyeonsan region, a range of properties representing unsaturated conditions were established through laboratory and field tests. Matric suction that reflects infiltration into soils is considered very important to analyze rainfall-induced landslides in this landscape. Therefore, the volumetric water content is estimated as a function of the matric suction of soil by laboratory tests and the initial matric suction is measured in the field. The soil water characteristic curve (SWCC), which represents the relationship between volumetric water content and matric suction, is a fundamental input parameter in the seepage analysis. For the seepage analysis, the input parameters such as unsaturated permeability, volumetric water content (dependent on matric suction) and initial matric suction for the soil (which governs the groundwater flow) have been derived from the soil-water characteristic curves of the soils. The SWCC and initial matric suction can be obtained by laboratory tests and field measurements. In this study, to obtain the SWCC of top soil on the Raemian watershed of the Umyeonsan region, a pressure plate extractor and filter paper tests were performed. The results of these tests are shown in Fig. 5. According to the Unified Soil Classification System (USCS), the top soil can be classified as SM (silty sand). The tested soil water characteristic curve showed an air entry value of 12 kPa, saturated volumetric water content was 50% and by the end of the desaturation, residual volumetric water content fell to 18%. In order to get the hydrogeological characteristics of the landslide, the matric suction is monitored with a jet-filled tensiometer (Gasmo et al., 1999). On the other hand, the osmotic suction was not measured.

In general, initial matric suction profiles are assumed to be linearly increasing above ground water table up to specified limiting values that are 200 kPa in clay, 70 kPa in silt, and 10 kPa in sand. (Ning Lu, 2004). Initial matric suction has a significant effect on the wetting band depth and groundwater table rising due to rainfall infiltration. In study area, the wetting band depth is changing 0.5 m by assuming initial matric suction that ranges from 70 to 200 kPa. Therefore, the monitoring and observing of field matric suction is essential. Fig. 6 shows a location of installed tensiometer. A total of 18 tensiometers were installed at different 6 locations (T1-T6) adjacent to the debris flow gullies (only the results for T1 and T5 are presented here). At each location, three tensiometers were embedded within the colluvial layer at depths of 0.3, 0.6 and 1.3 m below the ground surface. The matric suction values were measured for 45-day periods from June 29 to July 27, 2012. As show in Fig. 7 the matric

4

suction response to rainfall events at different locations and depths for T2 and T5. The initial matric suction was measured between 75 to 85 kPa at the site on June 29, 2012 prior to the rainy season. After the rainfall began, the matric suction within the colluvium rapidly decreased to 0 and 10 kPa at depths of 0.2 m (T5) and 0.3 m (T2), respectively. At depths of 0.9 m (T5) and 0.6 m (T2), the matric suction reduced to approximately 20 kPa which is the residual state of soil. At depths of 1.3 m (T2) and 1.4 m (T5), the matric suction remained at its initial value for five and six days, respectively. Such phenomena can be explained in that infiltrated water from rainfall had not yet reached these depths. After some period of time, due to additional rainfall occurring, matric suction finally decreased. The infiltration rate decreased with increasing depth from the ground. In the field measurement analysis, matric suction at 0.3 m was lower than colluvium located in a deeper layer due to the dominant effect of rainfall infiltration. This results implies that changes in matric suction due to rainfall infiltration increase both water content as well as the unsaturated permeability.

4 Results ~~and discussion~~

Both field and laboratory studies were conducted to determine the geotechnical, hydrogeological and vegetation characteristics and to investigate the geomorphological features and spatial distribution of the landslides. These included interpretation of aerial photographs, analysis of rainfall records, visual inspection and plant community survey.

4.1 Rainfall characteristics

The recorded rainfall data by two automatic rain gauges which in Seocho and Namhyun stations were used to assess landslide triggering rainfall conditions. The both stations are located at a distance of 2 km from the highest peak of the Umyeonsan region (Fig. 1).

The return period of rainfall intensities of this rainstorm for different durations were determined by applying the Gumbel distribution to the historical rainfall records of the Seoul observatory, where records had begun in 1961. The Seoul observatory is located at a distance of 11.7 km from the Umyeonsan peak.

According to the Korea Meteorological Administration, the average annual rainfall among Seoul is approximately 1450.5 mm, and during the summer season (June, July, August), a total of 892.1 mm of rainfall precipitation is recorded, which accounts for approximately 61% of the annual precipitation rate. It can be deduced that summer season constitutes a large portion of the annual rainfall.

Fig. 8 shows the hourly and cumulative rainfall for July 26 - 27, 2011 recorded at the rain gauges installed on the Namhyun station. The cumulative 24-h rainfall ending at 12:40 pm on 27 July 2011 was 425.5 mm (i.e., very heavy rainfall). The maximum hourly rainfall for the station was 112.5 mm, which occurred between 7:40 and 8:40 am on 27 July 2011. The 1-h rainfall registered at the Namhyun station was very severe, with a corresponding return period of more than 120 years. Interestingly, the peak hourly rainfall coincided well with the time triggering of the landslides at the Raemian watershed (starting at 8:30 pm).

5

The event occurred during July 26-27, 2011. Accumulation of rainfall during this period was unprecedented, which played a critical role in the landslide's occurrence. Rainfall intensity-duration thresholds (ID-curve method) are commonly used to predict the temporal occurrence of landslides. The thresholds represent the lower limit of peak rainfall intensities that induce landslides. Empirical ID thresholds are usually in the form of a power law equation (Guzzetti et al. 2008):

$$I = \alpha D^{\beta}, \tag{1}$$

where I is the rainfall intensity (mm/h), D is the duration (hour), and α and β are the empirical constants. Considering the duration of rainfall (16 h) prior to the Raemian landslide and the corresponding cumulative rainfall of 306.5 mm for the Namhyun station, the average rainfall intensity is 19.2 mm/h. For the Seocho station, the average rainfall intensity for the same duration is 16.0 mm/h. Fig. 9 indicates that the measured rainfall is not only beyond the metropolitan ID threshold curve of Seoul, located this study area, as suggested by Hong et al. (2017) but also exceeds international representative ID curves proposed by many researchers (Caine, 1980; Innes, 1983; Jan an Chen et al., 2005; Calcaterra and Sant, 2004; Dahal and Haswgawa, 2008; Guzzetti et al., 2008). Hence, the rainfall during this period was enough to trigger a landslide.

4.2 Vegetation characteristics

Vegetation, especially trees with root systems, plays a decisive role in slope stability, particularly on steep forested slopes liable to shallow rapid failures. The effect of vegetation on slope stability includes 1) mechanical stabilization of soil by roots and the surcharge from the self-weight of trees, and 2) soil water modification via evapotranspiration (Nilaweera and Nutalaya 1999). In shallow slopes, the tree roots may penetrate the entire soil mass, which acts as tensile elements within the soil matrix as well as anchors connecting weak soil into adjacent more stable soil. The root fiber reinforcement is highly variable, depending on the type and depth of soils and root characteristics controlled by species, edaphic and hydrological conditions (Wu and Sidle, 1995).

To explore the species distribution and structural diversity of vegetation communities, a field survey was conducted at the Raemian watershed, where a sampling plot of 400 m2, orientated parallel to the debris flow gully, was established. A total of 149 woody species were recorded: all living trees (the diameter at breast height, DBH > 0.06 m) were counted, and the characteristics of vegetation communities that include species, DBH, height and root depth were measured.

The Umyeonsan region is rich in flora. Species composition is dominated by Quercus mongolica (43%), known as Mongolian Oak. Since the Mongolian Oak grows fast, it has been widely used in the region for combating soil erosion as well as shallow landslides and debris flows. In the Umyeonsan region, dense understory vegetation (shrubs, bushes and herbs) with many well-branched stems within 2 m of the ground surface were sparsely distributed. The field survey also revealed that the root depths appear to be restricted to the surface layer of < 1 m, although the majority of colluvium depths in debris flows lie in the range of 1 to 2 m (Fig. 10). Typically, the presence of roots in soil reduce both water content and pore water pressures by the process of evapotranspiration and tree canopies, resulting in an increase of soil shear strength. However, the evapotranspiration and tree canopies are not influencing factors for landslides during the extensive rainy season. In the event of landslides occuring

in the Umyeonsan region, soils were saturated and evapotranspiration was low due to the high intensity storm. Consequently, a slight reduction in safety factor had been found in the Raemian watershed analysis (0.01 to 0.08). This result is in accordance with the previous phenomenological approach (Schmidi et al., 2001); it is well known that the self-weight, length and strength of tree roots have a close relationship with landslides. As confirmed in this study, such results were categorized as triggering mechanisms of the landslide.

4.3 Geotechnical characteristics

Ground investigation was performed to determine the geotechnical and hydrogeological properties of the initiation (landslide) and transportation areas of the debris flows. Five boreholes were drilled to confirm the stratigraphy previously described and to undertake in situ tests including standard penetration tests (SPT), saturated permeability tests and borehole shear tests. Six trial pits were also constructed to characterize the surficial materials that remained along the debris flow gullies. Both disturbed and undisturbed soil samples were obtained for laboratory tests.

The laboratory program to characterize the colluvial soil included the tests for the following: (1) soil classification (ASTM D2487-11); (2) water content (ASTM D4643-08); (3) Atterberg limits (ASTM D4318); (4) grain size distribution (ASTM D422-63); (5) soil-water characteristic curves (ASTM D6836-02, ASTM D5298-94); and (6) shear strength parameters from direct shear tests (ASTM D3080).

The soil investigation results are summarized in Table 1 and Table 2. Table 1 shows the results of the constant head permeability and shear tests in the boreholes. To best describe the in situ soil properties, shear tests in the borehole (STB) and constant head permeability were conducted, since it can rapidly determine a Mohr-Coulomb failure envelope and permeability in a borehole. Table 2 shows the results of laboratory soil tests performed to obtain the detailed information of slope failure at the Umyeonsan landslide in 2011. The direct shear test of the undisturbed soil samples indicates that the average strength parameters corresponded to a cohesion of 9.2 kPa and friction angle of 24.8°, which is similar to those from the in situ tests in the boreholes. The physical properties of the soil samples obtained from depths of 0.15–0.5 m in the colluvium are summarized. Such tabulated material properties of soil is reflected on the seepage analysis. Fig. 11 shows the locations of boreholes and seismic prospecting carried out within the watershed.

The geology from the borehole survey consists of distinct three layers, including a 1.5 - 4.5 m layer of colluvium, followed by a 0.5 - 9.9 m layer of highly weathered rock, and fresh rock (Fig. 12). The colluvial soils are made up of a wide range of particle sizes, characterized as silty sand. The gravel, cobbles and pebbles of various sizes are identified in colluvial deposits. Their shapes appear to be sub-angular to angular. The standard penetration number (N-value) of the colluvium is approximately 4/30 - 5/30. In general, N-values of less than 10 mean that the soil is very soft and loose (Bowles 1997). Therefore, it is inferred that the colluvial deposit provides the source material available for debris flows. The N-value of weathered rock widely varies from 12/30 to 50/10, depending on the degree of weathering. Based on the results of the constant head permeability and shear tests in boreholes, the permeability of the colluvium is approximately 10-4 m/s and the permeability of the weathered rock is of the order of 10-5 m/s.

7

The physical properties of the soil samples obtained from depths of 0.15 - 0.5 m in the colluvium are summarized as follows: The water contents ranges from 14.1 to 32.1%, indicating that the superficial layer is wet, with the soils having a high degree of saturation. The plastic and liquid limits of the soils are in the range of 20.9 to 23.8% and 30.2 to 42.1%, respectively. The colluvial deposits contain fines (i.e., silty and clay) of 28.8 - 55.7%, which help sustain high pore water pressure in the debris flow promoting travel (Iverson 2003). Ellen and Fleming (1987) analyzed the clay content of soil samples from colluvial slopes and demonstrated that the slope failure is significantly associated with a clay content of 8 to 25%. According to the Unified Soil Classification System (USCS), the colluvial soils are classified as SM and SC-CL.

5 Discussions

In this study, an integrated analysis methodology for rainfall-induced landslides was proposed by using a hydro-geotechnical coupled model that incorporates field matric suction in the slope stability analysis on large scale. This framework aims to estimate the actual scale of the landslide that occurred in the basin. Hence, in the process of investigating the trends of the wetting band depth and slope failure, coupled analysis of the transient seepage and slope stability were performed using SEEP/W and SLOPE/W (Geo-slope, 2012). The failure mechanism of these rainfall-induced landslides is influenced by the matric suction, which is a very important mechanism of the interpretation of the unsaturated of the soil. The initial groundwater table was assumed to be located at the top of the bedrock. The initial slope conditions were taken as hydrostatic with initial matric suction of 80 kPa obtained from field measurements and applied onto the subjected stratigraphy. Several soil properties are summarized in Table 3. For the purpose of validation of this modeling, the results of SEEP/W analysis were compared with the field matric suction monitoring (in Fig. 7). Fig. 13 shows the field matric suction distribution at 0.3 m, 0.7 m, and 1.1 m depths with dashed lines and the simulated matric suction at the same depth with solid lines. Average matric suction for four nodes in the target element is used in these comparisons. Stiffer responses of matric suction variation compared with those from field measurement are observed in the analysis. This indicates the limitation of the numerical analysis method used in this study. The complicated distribution of field matric suction, which depends on several surrounding circumstances, cannot be simply simulated through the numerical method in an idealized condition. Although the model has such limitations, the general trend of the measured matric suction is fairly well predicted. The depth from the slope surface affects the response of matric suction. When the infiltration distance is relatively long, it takes more time for the rainfall infiltration to arrive at a greater depth because rainfall flow on the slope surface is easily delayed in the small permeability of unsaturated soil.

The rainfall data recorded at the Seocho station was used as the flux boundary conditions, which is controlled at the surface of the slope. The total duration of rainfall from June 22 to July 27 was 850 h (35.4 days) and was divided into several stages to simulate a realistic rainfall event. In addition, a non-ponding boundary condition was adopted to prevent excessive accumulation of rainfall on the slope surface. The nodal flux of zero was applied along the sides and the base of the slope to simulate the no flow zone. Fig. 14 shows the finite element mesh and the boundary conditions .and results of pore water pressure distribution due to the infiltration analysis. The real-time rainfall data was applied to the surficial layer of the soil as

the hydraulic boundary condition. The bedrock was assumed to be relatively lower permeability which led to the conclusion that the bottom layer was impermeable.

Regarding the infiltration characteristics of the soil slope, a critical slip surface was evaluated to investigate slope instabilities and failure zones. Fig. 15 shows critical slip surfaces in the Raemian and Dukwooam watershed. The critical slip surface gradually deepens towards the bedrock with time during rainfall events. Fig. 16 shows the variations in the factor of safeties in the Raemian and Dukwooam watershed. The factor of safety of slopes for both watersheds decreased with time, reaching their minimum values at the end of the rainfall events. The initial factor of safety for the slope in Raemian watershed is 1.78 during the driest period, which is larger than that of the Dukwooam watershed (1.61) due to the different slope angles and soil depths. The factor of safety decreased significantly at the beginning of the rainfall events due to the effect of a reduction in matric suction. When rainwater infiltrated the soil layer, the matric suction decreased rapidly and the factor of safety also fell in response. The magnitude and the rate of decrease in the factor of safety is also related to the rainfall intensity. Fig. 17 depicts the change in the longitudinal profile before and after the landslide, the subjected Raemian watershed features a channel length of 632 m, a width of 30 - 40 m, and an average incised depth of 1.6 m of gully from the LiDAR survey.

The critical slip surface is consistently developed on the colluvium-bedrock interface at the end of the rainfall events, which shows good agreement with the actual failure zone (Fig. 15 and 17). Two types of landslides occurred in the Raemian watershed, and a series of landslides were triggered by subsurface infiltration and rising groundwater-table. In the Dukwooam watershed, the results of analysis for both relevant mechanisms reasonably agree with all of landslide observations. Because this site has a generally shallow soil depth of 2.0-3.0 m, it is sufficiently shallow with relation to the wetting band depth of 2.0 m in the test site. Thus, this area was exposed to the same level of landslide risk, which was triggered by subsurface infiltration and rising groundwater-table. The results show the primary triggering factors causing landslides, i.e., soil depth, and spatial and temporal distributions of groundwater variations.

As mentioned above, deficit matric suction is one of the most important variables for the analysis of rainfall-induced landslides. Rainfall-infiltration depth, known as a main triggering factor of a landslide, is a response by the initial matric suction and is affected by antecedent rainfall. It is difficult to analyze a rainfall-induced landslide for unsaturated soil slopes because all of the affecting aspects such as rainfall, initial matric suction and ground water level must be considered.

Consequently, based on this study, a hydro-geotechnical coupled analysis for rainfall-induced landslides was conducted. Such methodology determines the initial groundwater table sufficient to trigger slope failures, the change in the groundwater level due to rainfall infiltration and the rainfall-induced stability of slopes.

This methodology is based on experimental tests and numerical analyses which consider the important mechanism of partially saturated soil slopes due to deficit matric suction responding to rainfall. Fig. 19 shows the flow chart of integrated landslide analysis methodology in this study.

Step 1) Site investigations and experimental tests are carried out to obtain the index properties, unsaturated characteristics, , and rainfall characteristics at the site.

9

Step 2) The monitoring of field matric suction is performed to consider initial matric suction under dry period and antecedent rainfall effects under wet period, whereas a one-dimensional (1D) infiltration analysis should be conducted in the absence of measured data to determine the wetting band depth. For the 1D infiltration analysis, the site is modelled as a single column. A steady state seepage analysis is performed using pressure head boundary conditions for obtaining initial matric suction. To consider the influence of antecedent rainfall effects, the steady state seepage analysis is first performed to generate the initial condition in the site. A transient seepage analysis is then performed using real-time rainfall records. As a result, the calculated pore-water pressure distribution is considered as an initial state of the slope and used to calculate new pore-water pressure distributions in a two-dimensional (2D) seepage analysis.

Step 3-1) In the case of infinite slope failures, the wetting band depth in the targeted slope is calculated from the 1D seepage analysis. A slope stability analysis is conducted using the calculated wetting band depth to predict the shallow failure of the slope.

Step 3-2) In the case of rotational slope failures, the pore-water pressure distribution is determined through the 2D seepage analysis based on the initial condition obtained from the 1D infiltration analysis. A slope stability analysis is conducted with incorporation of the pore-water pressure distribution obtained from the 2D seepage analysis.

6 Conclusions

The overall objective of this study is to propose an integrated analysis methodology for the rainfall-induced landslide based on the comprehensive case study on the 2011 Umyeonsan (Mt.) and the monitoring of field matric suction. In addition, numerical analyses incorporated the important mechanism of partially saturated soil slopes due to deficit matric suction in response to rainfall. A framework for interpreting the complexities of actual scale landslides occurring in basins has been clearly demonstrated with the aid of hydro-geotechnical coupled modelling and experimental data. The following conclusions can be drawn from the findings of this study.

1) The landslide activity was primarily dependent on rainfall infiltration, soil properties, slope geometries, vegetations, and groundwater table positions. These were the relative importance factors in inducing instability of unsaturated soil slopes.

2) The integrated analysis methodology using the hydro-geotechnical coupled model was successfully developed to describe the unsaturated soil behavior of rainfall-induced landslides by linking seepage and deformation problems simultaneously. In particular, the proposed methodology with the incorporation of groundwater flow, rainfall infiltration into soils, and groundwater rising shows good agreement with the actual scrap zone.

3) The proposed methodology has clearly demonstrated that both shallow and deep-seated landslides, which means that these landslides were mainly governed by rainfall infiltration, groundwater rising. In addition, the two types of

10

landslide mechanisms show good agreement with the landslide observation, critical slip surface that tends to be expanded, and factor of safety that decreases due to prolonged rainfall.

Acknowledgments

5

11

References

Aman, A. A. and Bman, B. B.: The test article, J. Sci. Res., 12, 135–147, doi:10.1234/56789, 2015.

Bowel J.E.: Foundation analysis and design, fifth edn, McGraw-Hill, Singapore 1997.

Brinkgreve, R. and Swolfs, W.: PLAXIS 2D User's Manual, Plaxis. 2010.

5   Caine, N.: The rainfall intensity: duration control of shallow landslides and debris flows, Geografiska Annaler, Series A. Physical Geography, 23-27, 1980.

Capra, L., Lugo-Hubp, J., and Borselli, L.: Mass movement in tropical volcanic terrains: the case of Teziutlan, Engineering Geology, 69, 357-379, 2003.

Cascini, L., Cuomo, S., Pastor, M., and Sorbino, G.: Modeling of Rainfall-Induce Shallow Landslides of the Flow-Type, 10   Journal of geotechnical and geoenvironmental engineering, 136(1), 85-98, 2010.

Chen, L., & Young, M. H.: Green-Ampt infiltration model for sloping surfaces, Water Resources Research, 42(7), 2006.

Dahal, R. K., Hasegawa, S., Nonomura, A., Yamanaka, M., Masuda, T., & Nishino, K.: GIS-based weights-of-evidence modelling of rainfall-induced landslides in small catchments for landslide susceptibility mapping, Environmental Geology, 54(2), 311-324, 2008.

15   Ekanayake, J. C., and Phillps, C. J.: Slope stability thresholds for vegetated hillslopes: a composite model, Canadian geotechnical journal, 39, 849-862, 2002.

Ellen S.D., Fleming R.W.: Mobilization of debris flows form soil slips, San Francisco Bay Region, California, Reviews in Engineering Geology, 7, 31-40, 1987.

Fourie, A.B., Rowe, D., Blight, G.E.: The effect of infiltration on the stability of the slopes of a dry ash dump, Geotechnique, 20   49 (1), 1 – 13 1999.

Fredlund, D.G., Rahardjo, H, Fredlund, M.D.: Unsaturated soil mechanics in engineering practice, John Wiley & Sons, 2012.

Fuchu D., Lee C.F., Sijing W.: Analysis of rainstorm-induced slide-debris flows on natural terrain of Lantau Island, Hong Kong." Engineering Geology, 51, 279-290, 1999.

Fuchu, D., Lee, C. F., and Sijing, W.: Analysis of rainstorm-induced slide-debris flows on natural terrain of Lantau Island, 25   Hong Kong, Engineering geology, 51, 279-290, 1999.

GEO-SLOPE.: User's Manual, Geo-Slope International Ltd. Calgary, Alberta, Canada, 2012.

Godt J.W., Coe J.A.: Alpine debris flows triggered by a 28 July 1999 thunderstorm in the central Front Range Colorado, Geomorphology, 84, 80-97, 2007.

Guzzetti, F., Peruccacci, S., Rossi, M., & Stark, C. P.: The rainfall intensity–duration control of shallow landslides and debris 30   flows: an update." Landslides, 5(1), 3-17 2008.

Hungr, O., Evans, S. G., Bovis, M. J., and Hutchinson, J. N.: A review of the classification of landslides of the flow type, Environmental & Engineering geoscience, 7(1), 221-238, 2001.

Innes, J. L.: Debris flows. Progress in physical geography, 7(4), 469-501, 1983.

12

Iverson R.M.: The debris-flow rheology myth, Debris flow hazards mitigation: mechanics, prediction, and assessment. 1, 303-314, 2003.

Iverson, R. M.: Landslide triggering by rain infiltration, Water resources research, 36(7), 1897-1910, 2000.

Jeong, S., Kim, J. & Lee, K.: Effect of clay content on well-graded sands due to infiltration, Engineering Geology, 102, 74-81, 2008.

Kim J., Jeong S., Park S., Sharma J.: Influence of rainfall-induced wetting on the stability of slopes in weathered soils, Engineering Geology, 75, 251-262, 2004.

Kim J., Jeong S., Regueiro R.A.: Instability of partially saturated soil slopes due to alteration of rainfall pattern, Engineering Geology, 147, 28-36, 2012.

Kim, J., Lee, K., Jeong, S., & Kim, G.: GIS-based prediction method of landslide susceptibility using a rainfall infiltration-groundwater flow model, Engineering Geology, 182, 63-78, 2014.

Kim, Y. M., Jeong, S.: Modeling of shallow landslides in an unsaturated soil slope using a coupled model, Geomechanics and Engineering, 13(2), 353-370, 2017.

Kim, Y. M., Jeong, S., & Kim, J.: Coupled infiltration model of unsaturated porous media for steady rainfall, Soils and Foundations, 56(6), 1071-1081, 2016.Korea forest research institute (KFRI).: Standard manual for forest biomass investigation, 2006.

Korean Geotechnical Society (KGS).: Research contract report: addition and complement causes survey of Umyeonsan (Mt.) landslide, 2012.

Le T., Bae D.H.: Evaluating the utility of IPSS AR4 GCMs for hydrological application in South Korea, Water Resource Management, 27, 3227-3246, 2013.

Li, A. G., Yue, Z. Q., Tham, L. G., Lee, C. F., & Law, K. T.: Field-monitored variations of soil moisture and matric suction in a saprolite slope, Canadian Geotechnical Journal, 42(1), 13-26, 2005.

Lu N., Godt J.: Infinite slope stability under steady unsaturated seepage conditions, Water Resources Research, 44, 11, 2008.

Lu N., Likos W.J.: Unsaturated soil mechanics. John Wiley & Sons, New Jersey, 2004.

Lu, N., and Likos:, W.J.: Unsaturated Soil Mechanics, John Wiley and Sons, New Jersey, 2004.

Lutenegger, A. J., & Miller, G. A.: Uplift capacity of small-diameter drilled shafts from in situ tests, Journal of geotechnical engineering, 120(8), 1362-1380, 1994.

Ng, C. W. W., & Shi, Q.: A numerical investigation of the stability of unsaturated soil slopes subjected to transient seepage, Computers and geotechnics, 22(1), 1-28, 1998.

Ng, C.W.W., Springman, S.M. Alonso, E.E.: Monitoring the Performance of Unsaturated Soil Slopes, Geotechnical and Geological Engineering, 26, 799-816, 2008.

Ng. C.W.W., Zhan, L.T., Bao, C.G., Fredlund, D.G., Gong, B.W.: Performance of an Unsaturated Expansive Soil Slope Subjected to Artificial Rainfall Infiltration, Géotechnique, 53, 143-157, 2003.

13

Nilaweera N.S., Nutalaya P.: Role of tree roots in slope stabilization, Bulletin of Engineering Geology and the environment, 57, 337-342, 1999.

Park, D. W., Nikhil, N. V., and Lee, S. R.: Landslide and debris flow susceptibility zonation using TRIGRS for the 2011 Seoul landslide event, Natural hazards and Earth system sciences, 13, 2833-2849, 2013.

5   Pirone M, Papa R, Nicotera MV.: Test site experience on mechanisms triggering mudflows in unsaturated pyroclastic soils in southern Italy, Proceedings of the 5th International Conference on Unsaturated Soils, Taylor & Francis, UK, 2, 1273–1278, 2011.

Rahardjo, H., Leong, E.C., Gasmo, J.M., and Tang, S.K.: Assessment of rainfall effects on stability of residual soil slopes, Proc. 2nd International Conference on Unsaturated Soils, Beijing, China, 2, 280-285, 1998.

10   Sorbino, G., & Nicotera, M. V., Unsaturated soil mechanics in rainfall-induced flow landslides, Engineering Geology, 165, 105-132, 2013.

Take, W. A., Bolton, M. D., Wong, P. C. P., Yeung, F. J.: Evaluation of landslide triggering mechanisms in model fill slopes, Landslides, 1(3), 173-184, 2004.

Tiranti D., Bonetto S., Mandrone G.: Quantitative basin characterization to refine debris-flow triggering criteria and processes:

15   an example from the Italian Western Alps, Landslides, 5, 45-57, 2008.

Wang, F. W., Sassa, K., and Wang, G.: Mechanism of a long-runout landslide triggered by the August 1998 heavy rainfall in Fukushima Prefecture, Japan., Engineering Geology, 63, 169-185, 2002.

Wu W., Sidle R.C.: A distributed slope stability model for steep forested basins, Water Resources Research, 31, 2097–2110, 1995.

20   Yang, D. Q., Rahardjo, H., Leong, E. C., and Choa, V.: Coupled model for heat moisture air flow and deformation problems in unsaturated soils, Journal of engineering mechanics, 124(12), 1331-1338, 1998.

14
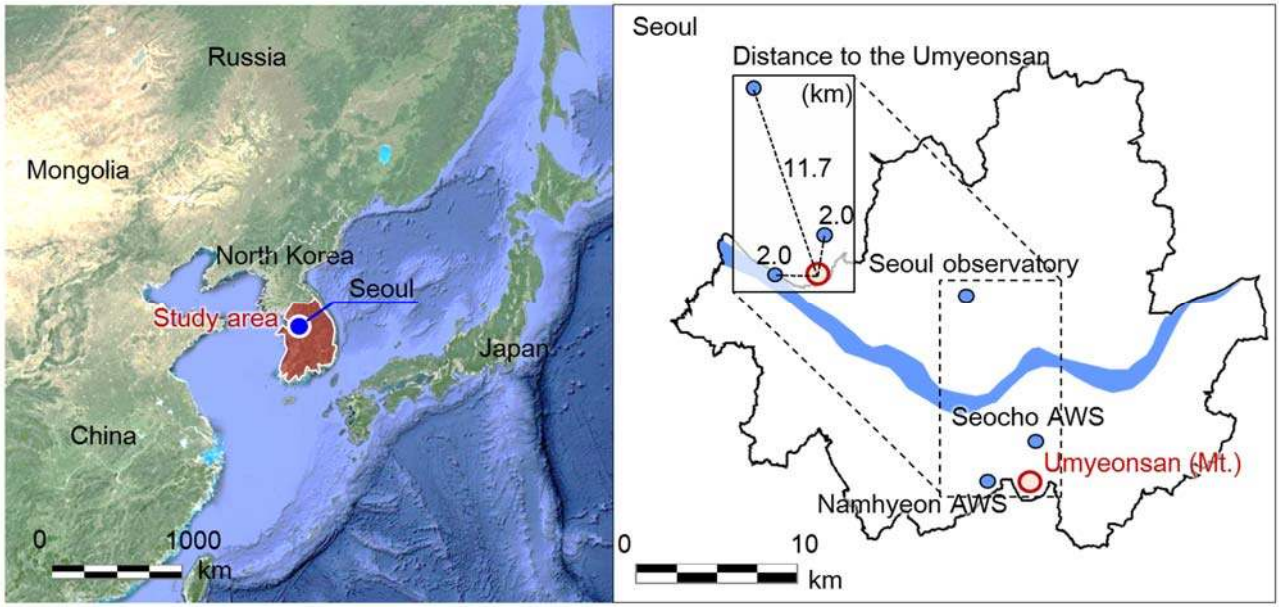
Figure 1: Location of the Umyeonsan (Mt.) landslides in Seoul, Korea
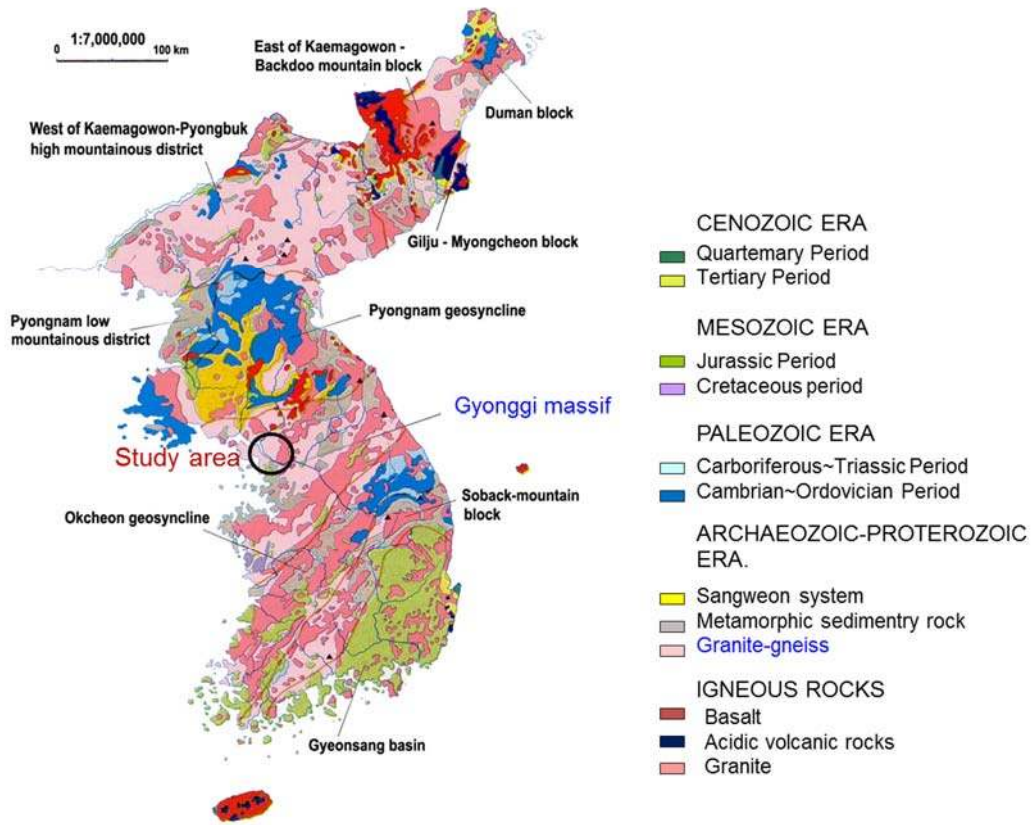
Figure 2: Geological Map of Korea Peninsula
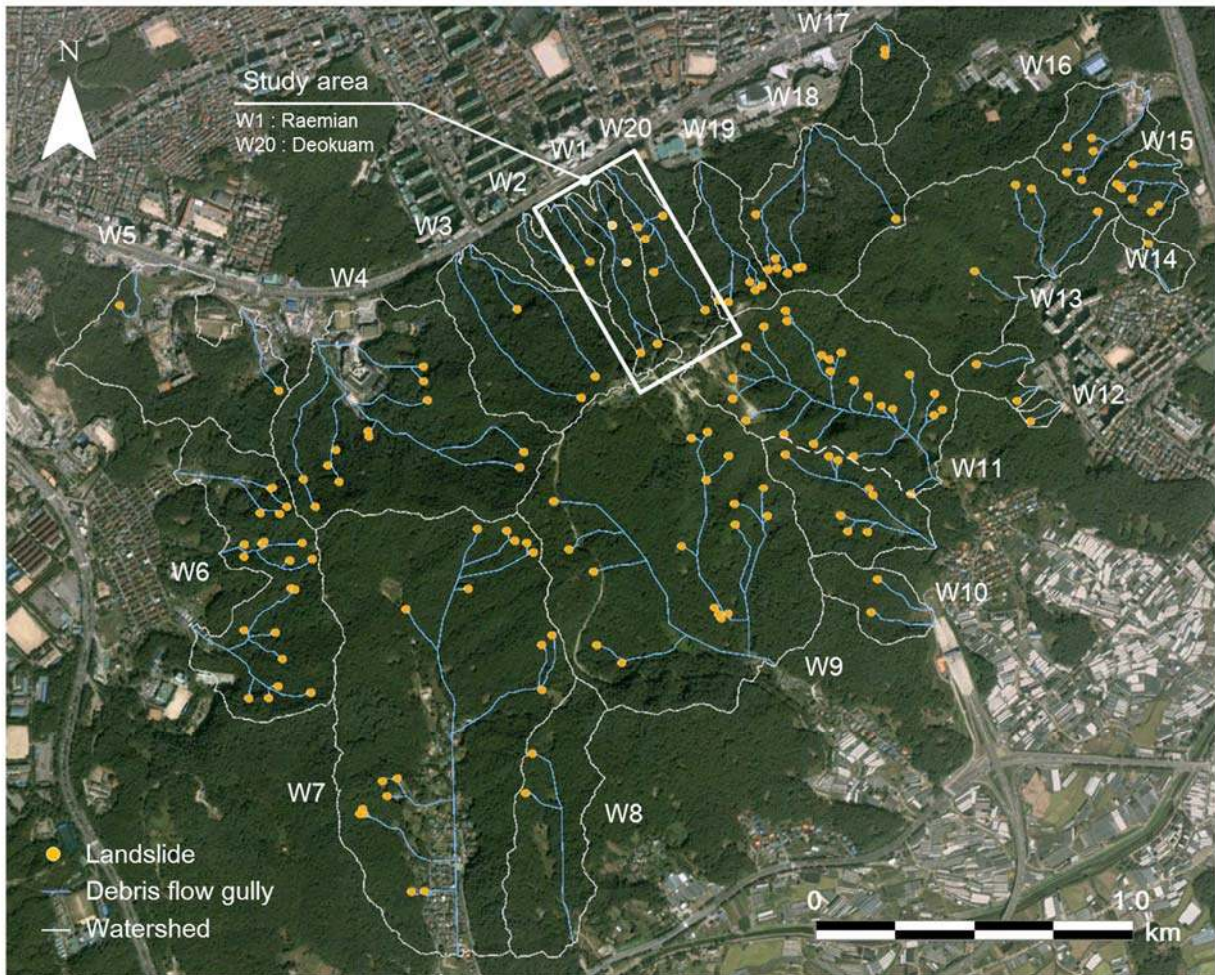
Figure 3: Satellite image showing 33 debris flow gullies (marked in blue), watersheds (outlined by white lines), and 151 landslides (modified from Korean Geotechnical Society, 2012).
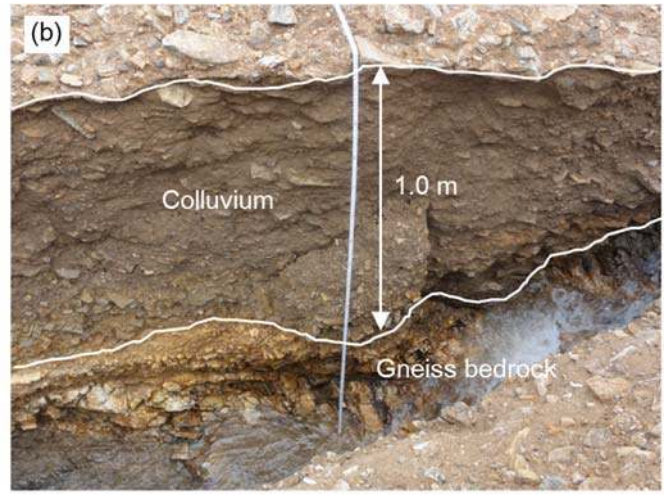
Figure 4: Photographs taken at the initiation, transportation and deposition areas of debris flows.
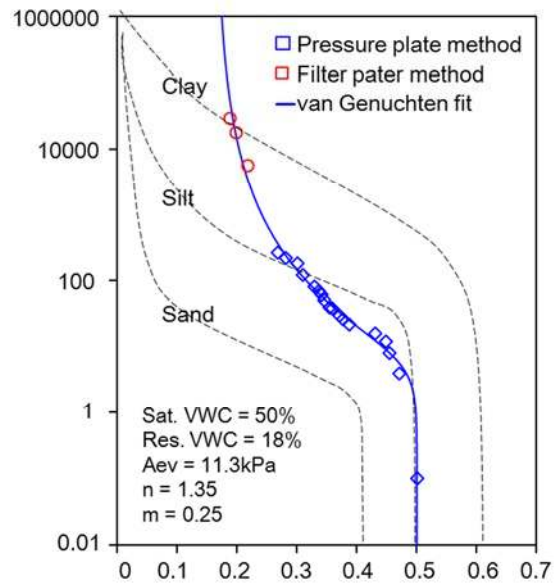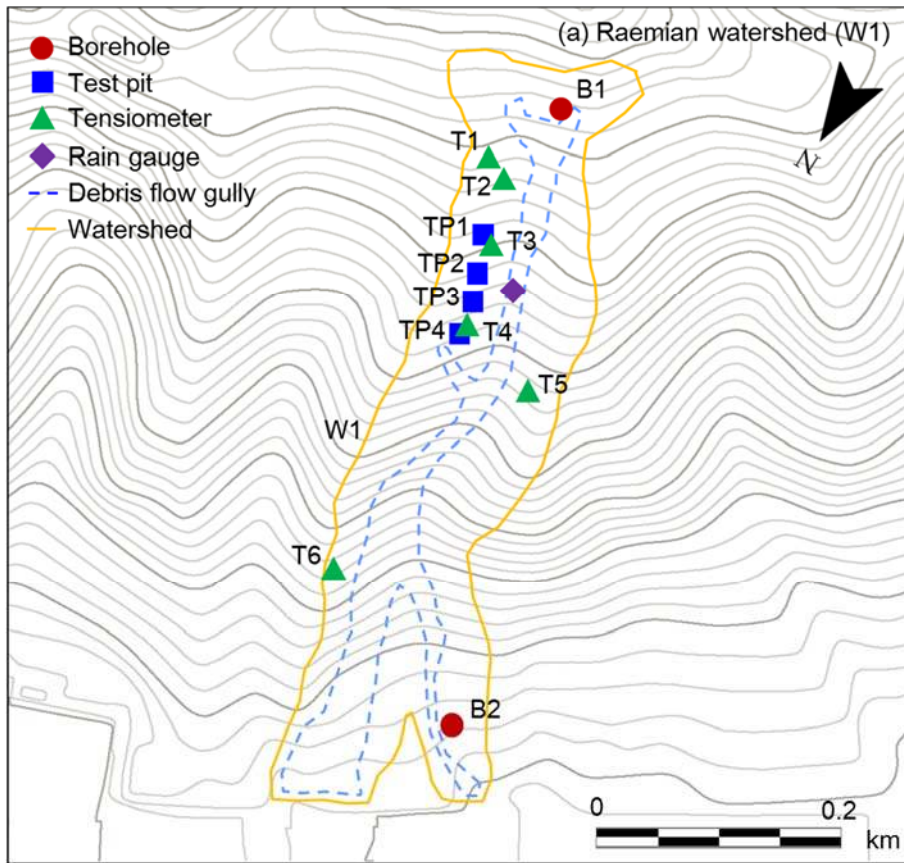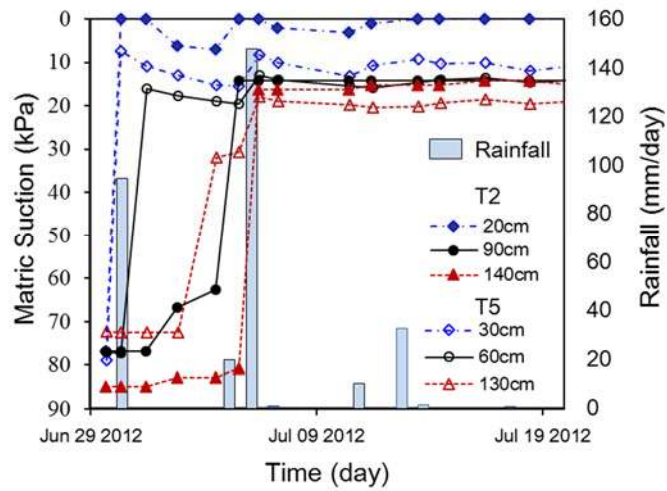
Figure 5: Soil-water characteristic curves.

Figure 6: Location map of boreholes, test pits and matric suction of monitoring site.

5   **Figure 7: Results of measured matric suction and rainfall data (T2, T5).**
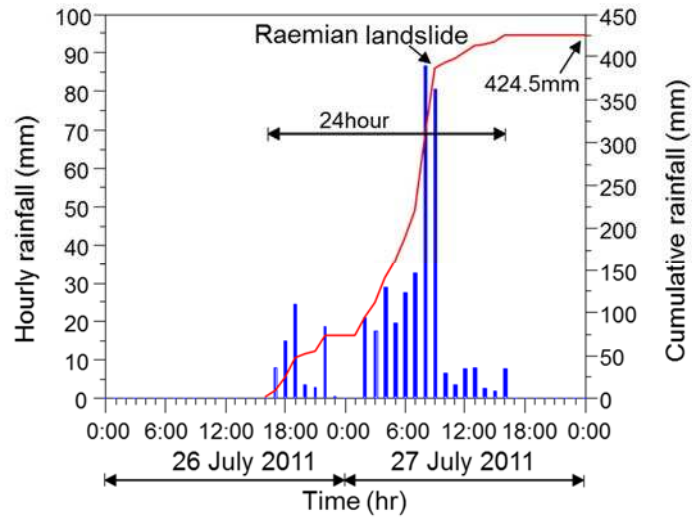
Figure 8: Hourly and cumulative rainfall of 26-27 July 2011 at Namhyun station.
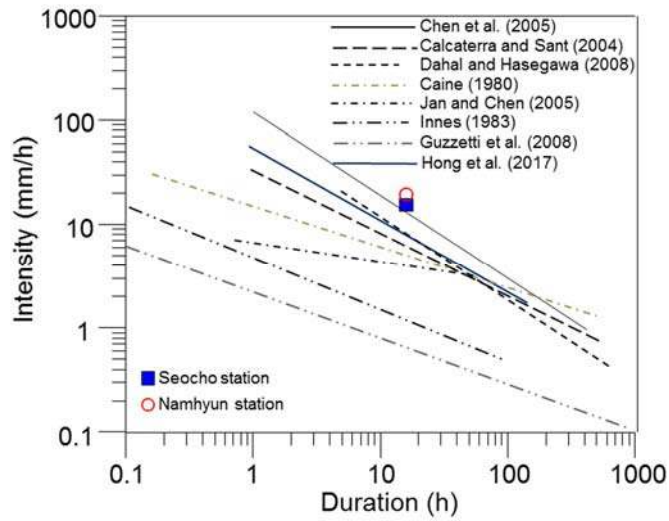
5

Figure 9: Comparison of measured rainfall intensity-duration data and existing intensity-duration threshold curves.

21
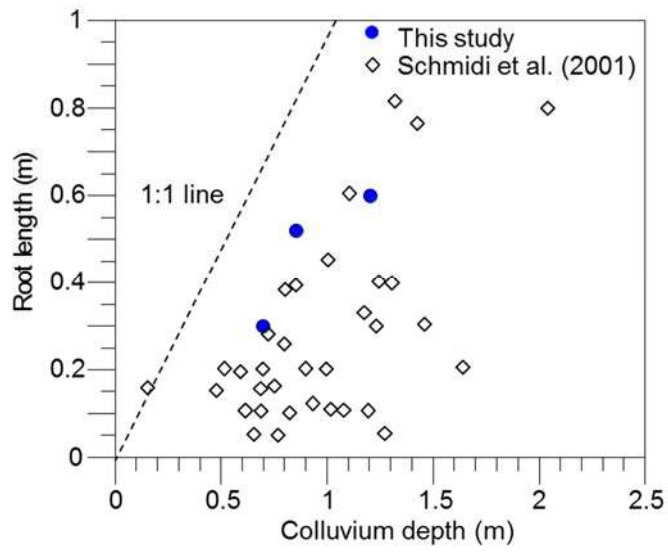
Figure 10: Relationship between root length and colluvium depth.
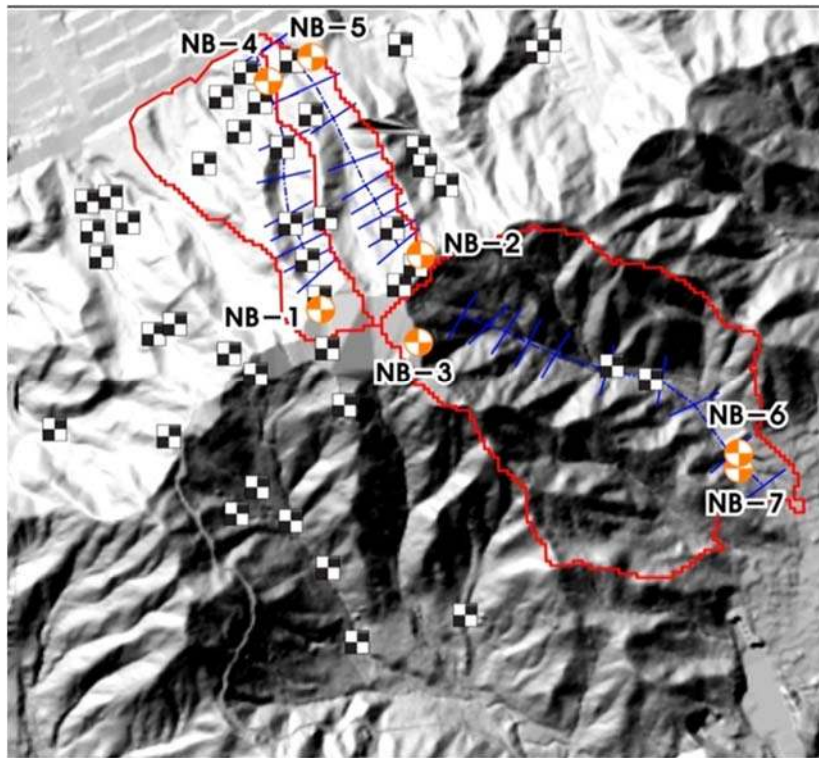
5   **Figure 11: Location plan of ground investigations (Korean Geotechnical Society, 2012).**
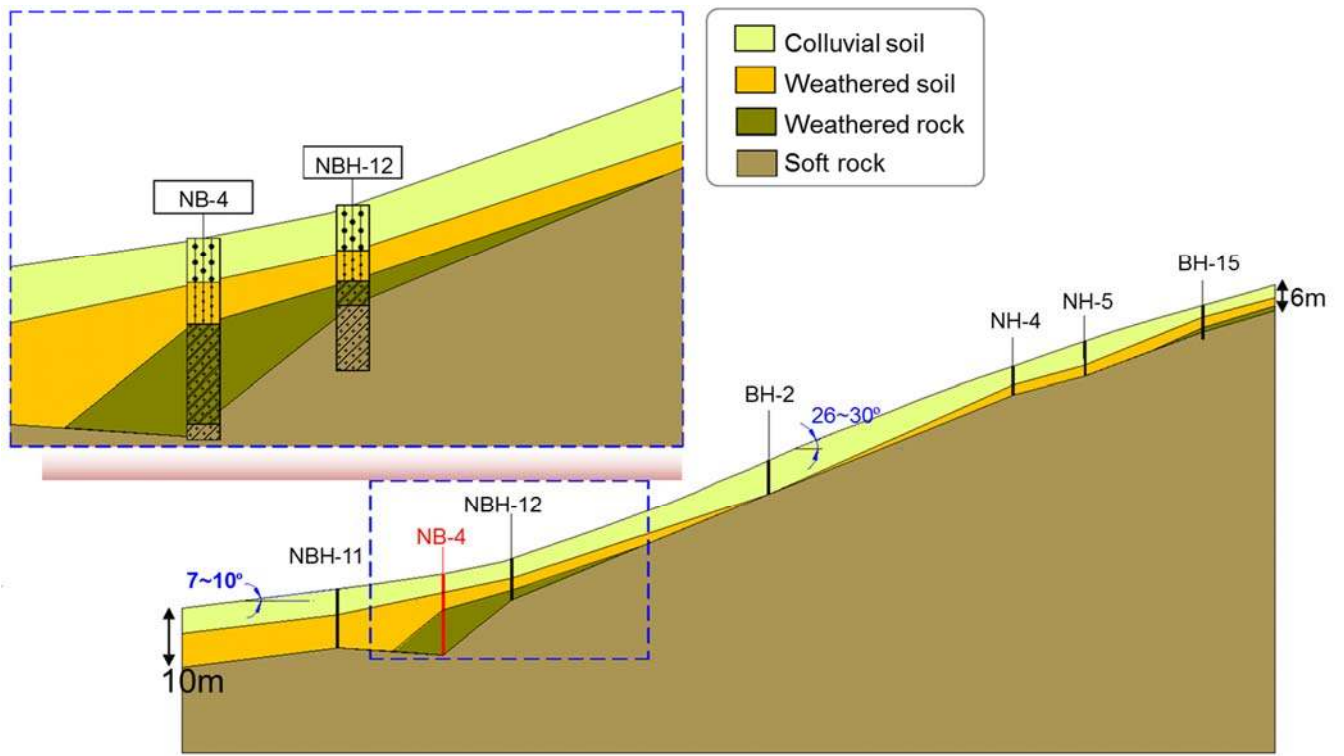
(a) Typical soil profile of Umyeonsan
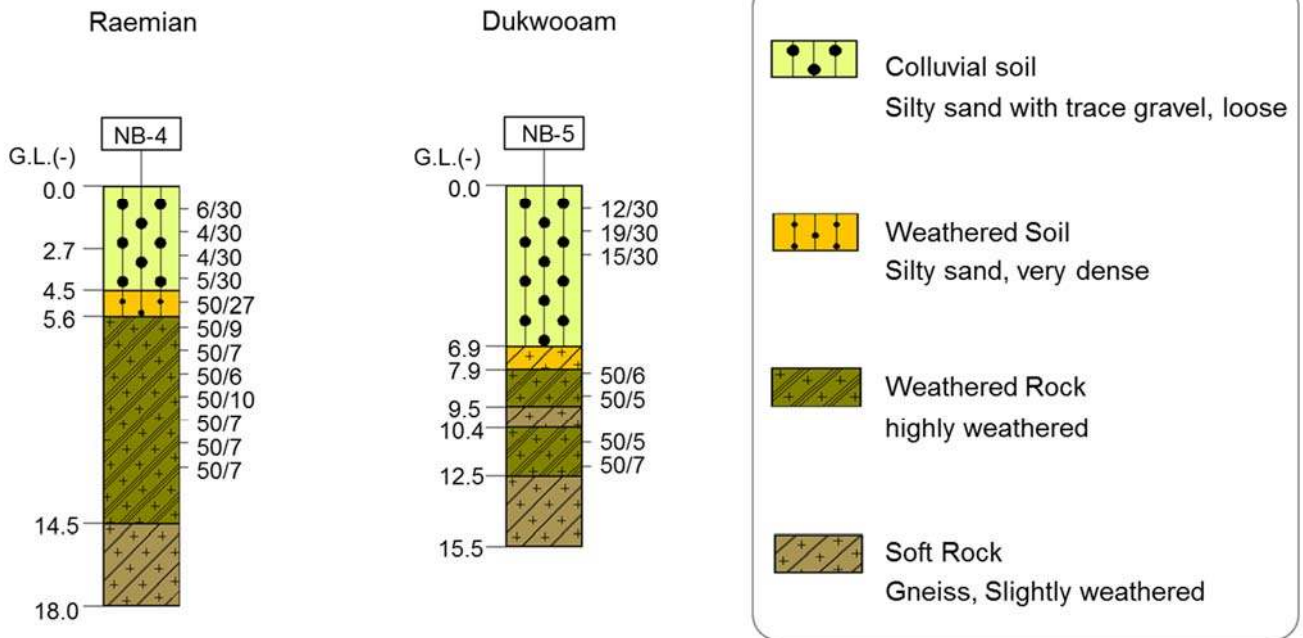
(b) Representative soil profiles of two watersheds

Figure 12: Soil profiles of the studied area.

5
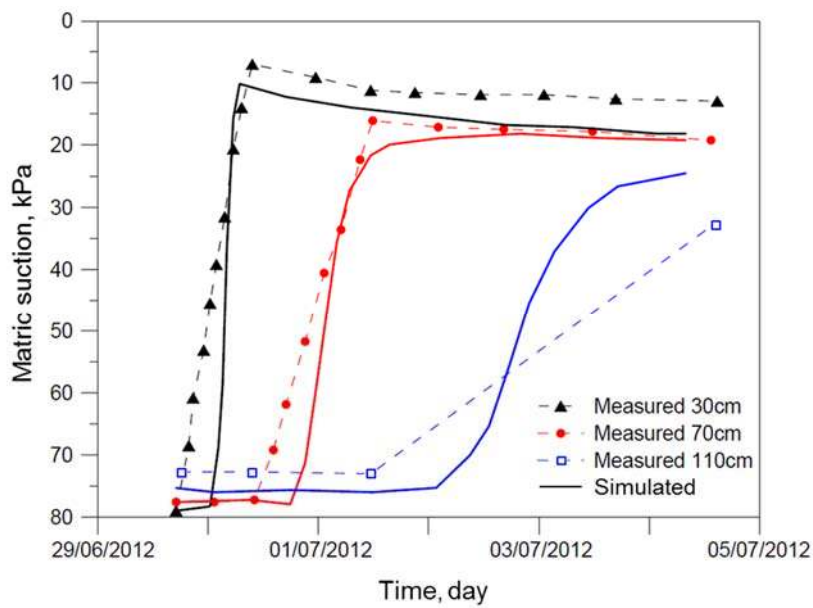
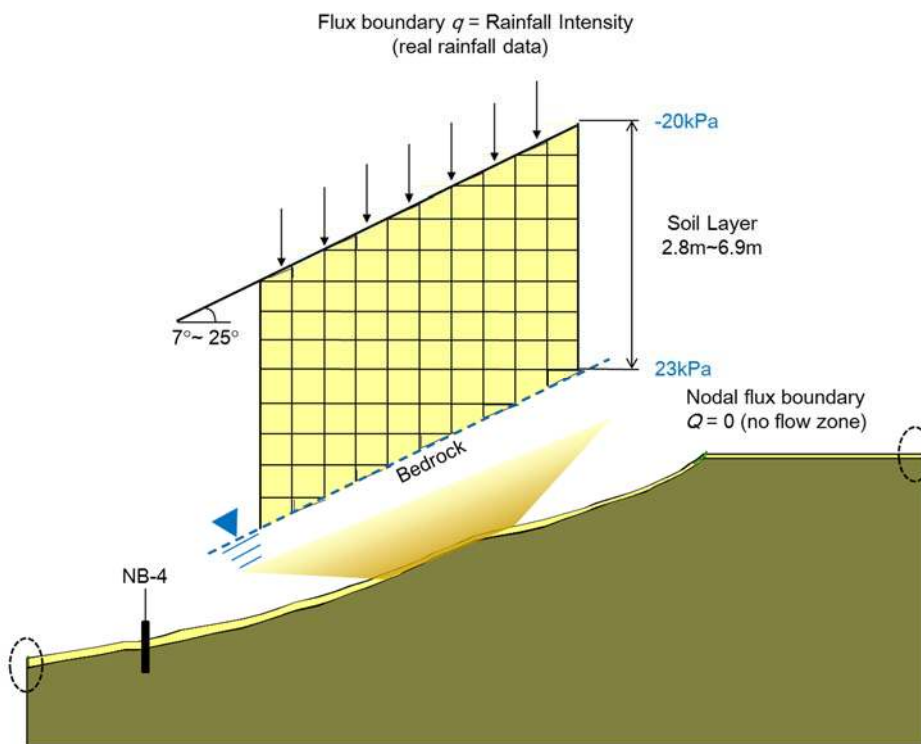**Figure 13: Comparison between measured and predicted matric suction.**
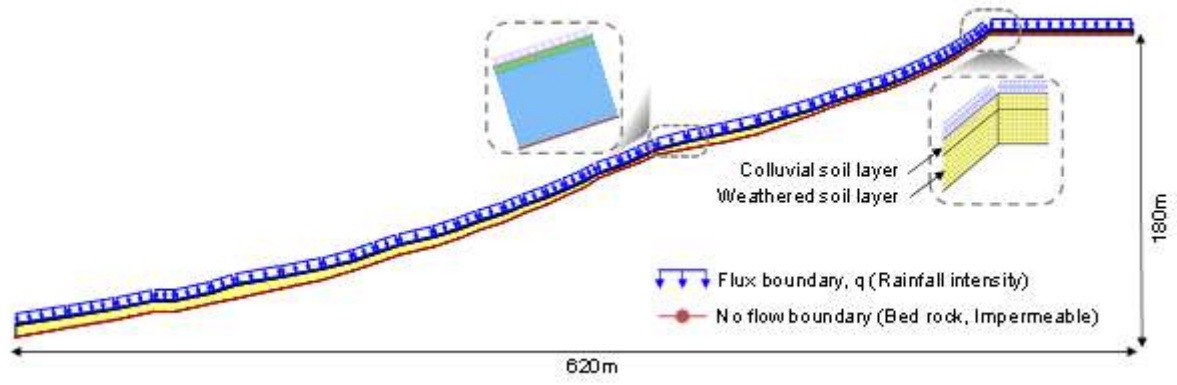
Figure 14: Soil slope mesh and boundary conditions used in two-dimensional seepage analysis, and results of pore-water pressure distributions.
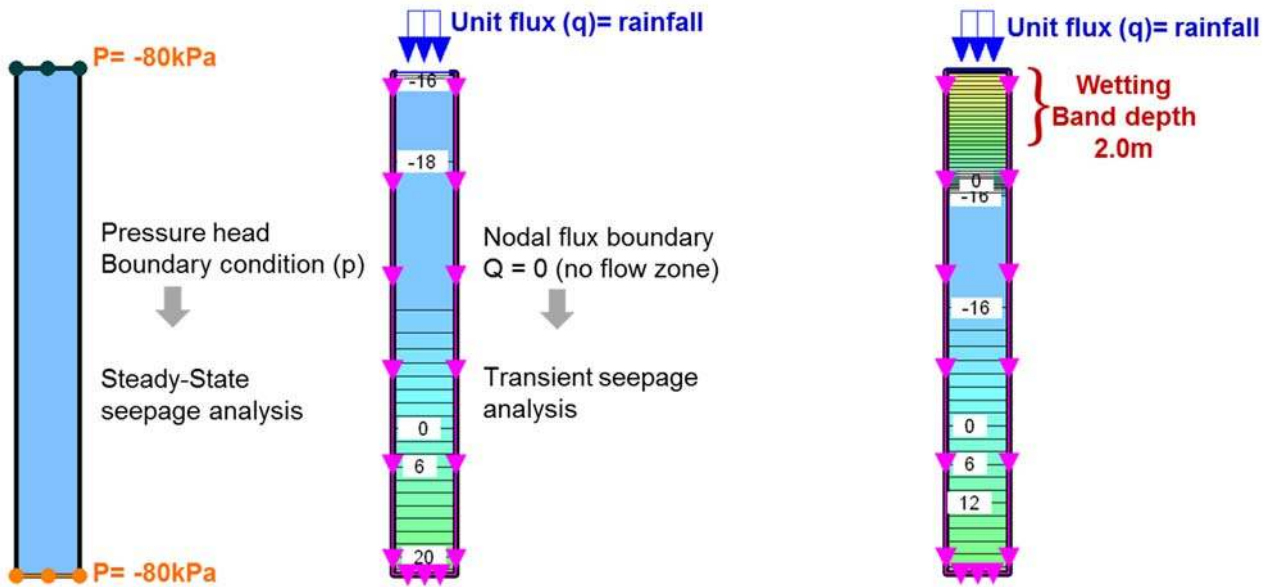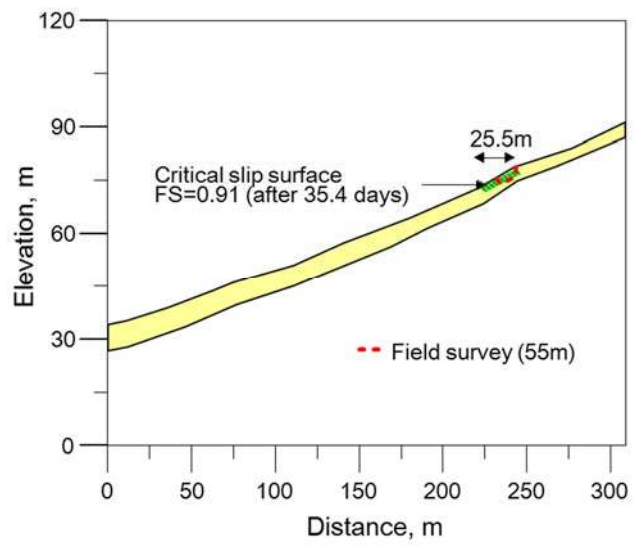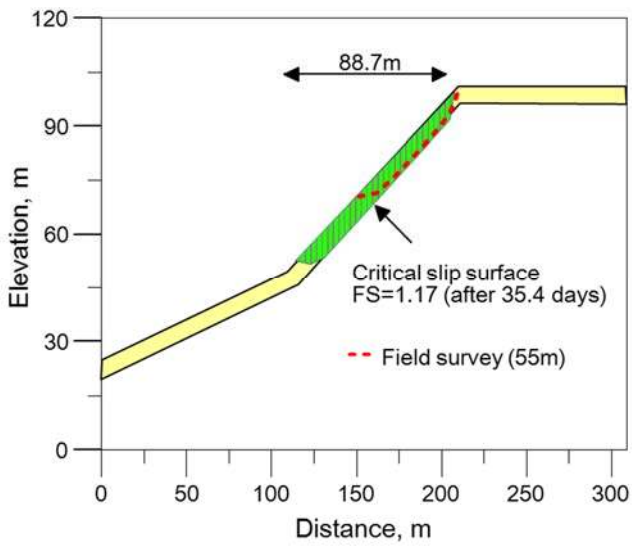
(a) Initial hydraulic conditions for 1D and 2D seepage analysis (b) 1D seepage analysis for assessing shallow failures
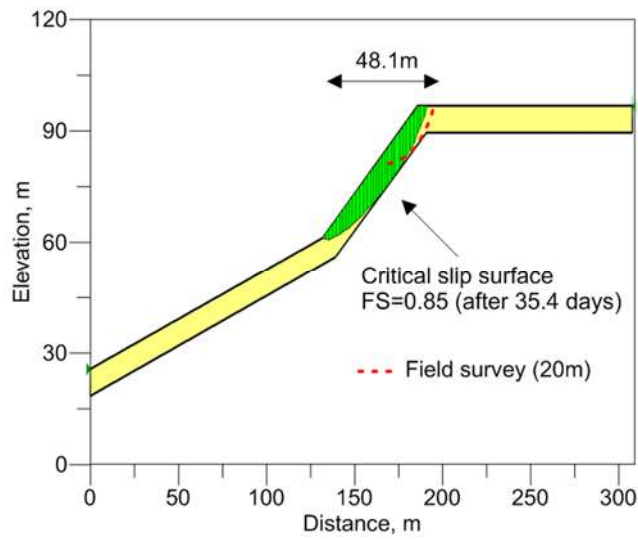

(c) 2D seepage analysis for assessing deep-seated failures

5   **Figure 14: Procedure of numerical modeling for assessing shallow and deep-seated failures.**

26

(a) Raemian watershed

5

(b) Dukwooam watershed

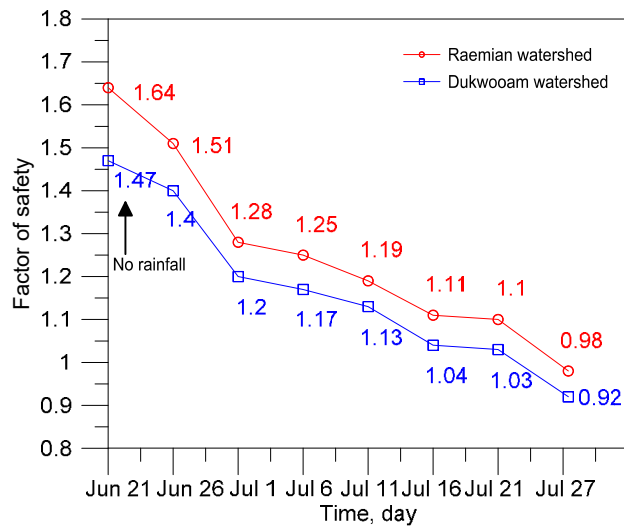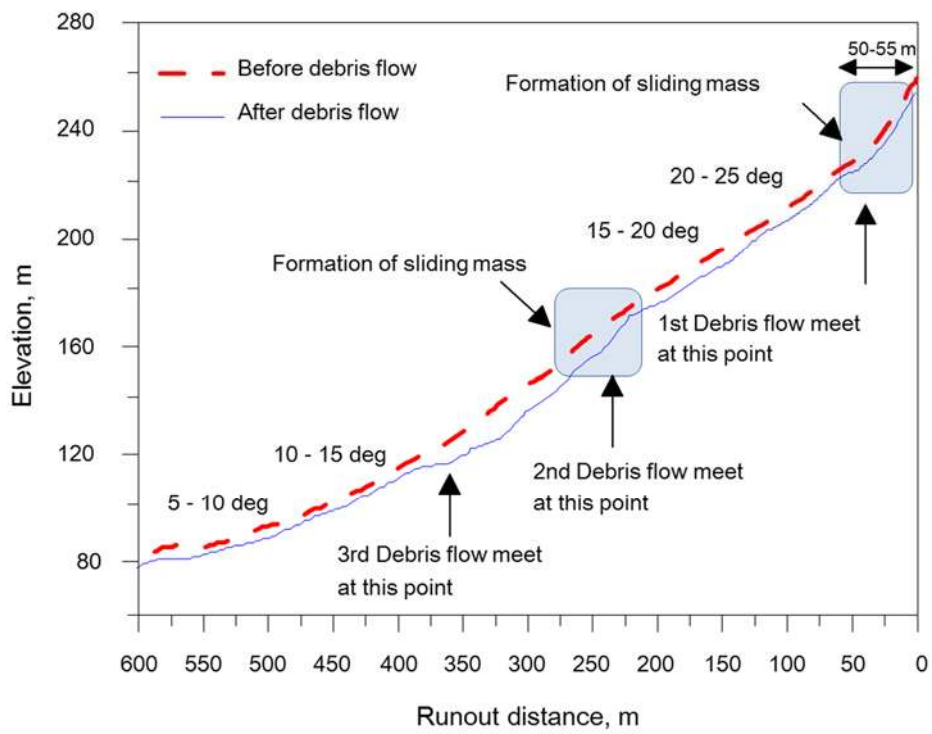**Figure 15: Critical slip surface from coupled analysis.**

Figure 16: Variation in factor of safety at studied areas with time.

5   **Figure 17: Longitudinal profile of debris flow gully from LiDAR survey in Raemian watershed.**
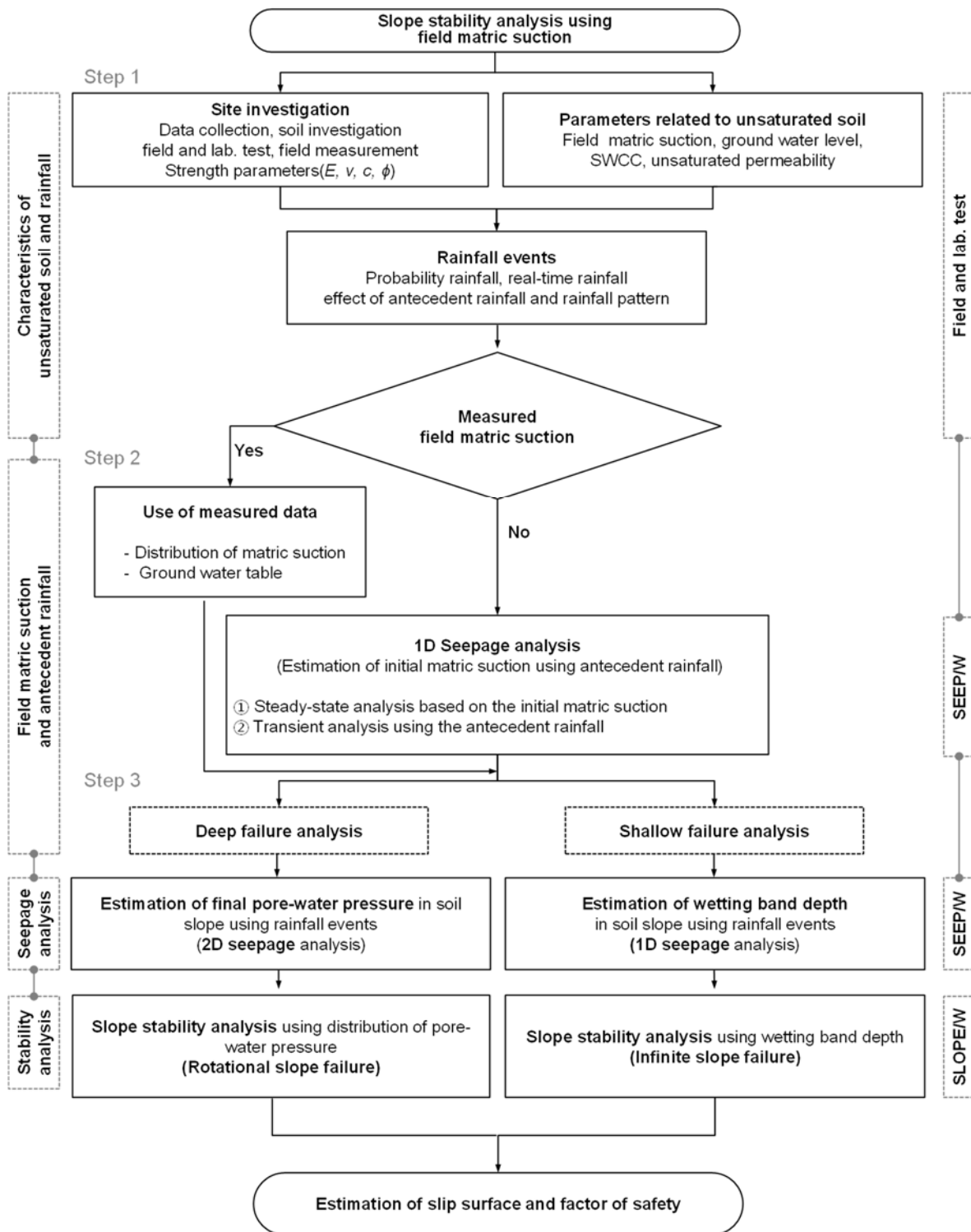
28

Figure 18: Flow chart of integrated landslide analysis methodology.

Table 1 In situ permeability and shear strength of the soil obtained from constant head permeability and shear tests performed in boreholes

Borehole	Depth (m)	Soil type	k (m/s)	c (kPa)	ϕ (°)
B-1	1 - 2	Colluvium	4.67×10^{-6}	7.5	22.3
B-2	3 - 4	Colluvium	8.08×10^{-6}	6.9	25.1
	5 - 6	Weathered rock	1.99×10^{-6}	18.1	27.3
B-3	1 - 2	Colluvium	8.08×10^{-4}	8.36	24.78
	3 - 4	Weathered soil	1.02×10^{-4}	18.55	28.22
B-4	2 - 3	Colluvium	7.92×10^{-4}	11.89	27.01
	8 - 9	Colluvium	9.55×10^{-5}	14.96	32.13

Note: k is the permeability; c is the apparent cohesion; ϕ is the internal friction angle.

Table 2 Index properties of the colluvial deposit from laboratory tests

Test pit	Depth (m)	w (%)	PL (%)	LL (%)	% Fines	USCS	c (kPa)	ϕ (°)
TP-1	0.5	18.2	21.2	36.6	51.9	CL	9.2	21.7
TP-2	0.5	14.1	22.3	31.6	28.9	SC	10.9	23.7
TP-3	0.5	32.1	23.7	40.6	55.7	CL	11.3	23.1
TP-4	0.5	15.8	20.9	35.9	44.4	SC	11.8	22.7

Note: w is the water content; PL is the plastic limit; LL is the liquid limit; % Fines < 0.075 mm; USCS is the Unified Soil Classification System; c is the soil cohesion; ϕ is the soil friction angle.

Table 3. Mechanical and hydraulic properties of the soil used in this study

Parameters	Values[*]	Description
Hydraulic conductivity, k_s	8×10^{-6} m/sec (28.8 mm/h)	in situ permeability test
Initial water contents, θ_i	28.0~32.0 (30.0) %	SWCC test
Water-content deficit, $\Delta \theta$	0.20	SWCC test
Wetting front suction head, ψ_f	830 mm	SWCC test
Soil cohesion, c_s'	6.9~18.5 (11.7) kPa	direct shear test, borehole shear test
Soil friction angle, φ'	21.7~32.1 (25.3°) °	direct shear test, borehole shear test
Total unit weight of soil, γ_t	17.0~18.5 (18.0) kN/m³	laboratory density test
Additional shear strength by roots of tree, c_r'	1.0 kPa	suggested by Norris (2008)
Uniform load by tree, q_0	0.253 kPa	suggested by KFRI (2006)

[*] () is number of average